DIFFUSION COEFFICIENTS OF HEMOGLOBIN BY INTENSITY FLUCTUATION SPECTROSCOPY

EFFECTS OF VARYING pH AND IONIC STRENGTH

K. J. LAGATTUTA, *Department of Physics, University of Connecticut, Storrs, Connecticut 06268*
V. S. SHARMA, *Department of Medicine, University of California at San Diego, La Jolla, California 92093*
D. F. NICOLI, *Department of Physics, University of California at Santa Barbara, Santa Barbara, California 93106*
B. K. KOTHARI, *Carnegie Institute of Washington, Washington, D.C. 20015 U.S.A.*

ABSTRACT Measurements of the mutual diffusion coefficients (D) of the liganded human hemoglobins (Hb) oxy-HbA and oxy-HbS were performed as a function of Hb concentration (CHb), pH, and ionic strength (Γ) by intensity fluctuation spectroscopy (IFS). Average diffusion coefficients, $\langle D \rangle$, and normalized variances, $\langle (D/\langle D \rangle - 1)^2 \rangle$, were recorded. Results are reported and select features are discussed quantitatively. (*a*) for $\Gamma = 0.15$ M, the shape of the $\langle D \rangle$ vs. CHb curve is found to vary with pH. We develop a precise description of this effect in the form of an algebraic relationship between $\langle D \rangle$, CHb, and Z, the titration charge. (*b*) only slight differences between the $\langle D \rangle$ values of oxy-HbS and oxy-HbA are observed, at $\Gamma = 0.15$ M, for CHb $\lesssim$ 10 g%. These differences are explained by the theory of part *a*. (*c*) No evidence of aggregation is found in solutions of oxy-HbA or oxy-HbS, at $\Gamma = 0.15$ M, for CHb $\lesssim$ 10 g%. (*d*) Indications of aggregation appear in oxy-HbA solutions at very low concentrations of salt. An estimate is made of the extent of aggregation, and the average radius of a cluster is determined.

1. INTRODUCTION

A. General

We report the results of new measurements of the mutual diffusion coefficients of the liganded human hemoglobins oxy-HbA and oxy-HbS by intensity fluctuation spectroscopy (IFS). All work was performed on materials in aqueous solution and falls into two groups. The first group consists of measurements made in the presence of phosphate buffers at fixed ionic strength, $\Gamma = 0.15$ M, and with the pH varying between 6.3 and 7.4; i.e., with the pH varying from well below to well above the iso-electric point (pI) of these two proteins. (The pI's of oxy-HbA and oxy-HbS are 6.9 and 7.1, respectively [1]. In this group, Γ has its in vivo value.) The second group consists of measurements made at pH $\simeq$ 6.7 and with the ionic strength varying between 1 mM and 3 M. Throughout, major emphasis was placed upon the study of oxy-HbA, as we thought it necessary to gain a more complete understanding of IFS measurements on this most common system first.

The remainder of this paper has been organized as follows: in section 1B we provide background for the problem and review relevant features of the IFS method; in section 2 we

describe our sample preparation and IFS measurement technique; in section 3 we tabulate and discuss our results; and in section 4 we give our conclusions.

B. Background

BA. THE PROBLEM For some time now the mechanism of the in vitro gelling of human sickling hemoglobin (HbS) has been a subject of widespread interest and intense study (2). It was supposed that a knowledge of the steps leading to the formation and stabilization of the gel, in vitro, would facilitate design of therapies aimed at disrupting the gelling process, and/or the gel state, in vivo (3). The ultimate alleviation of those life-threatening and painful symptoms attending sickle crises (2) in patients homozygous for the mutant Hb β-chain has motivated much or all of this research. But, in spite of the large body of information that has been accumulated by different workers using a variety of experimental techniques, the goal has not yet been reached. Perhaps the reason for this is that present understanding of the gelling process is still rather superficial.

The detailed intermolecular interactions responsible for the stabilization of the gel are only now just beginning to be discovered (4, 5), even though the structure of the Hb molecule has been known for several years. Of perhaps equal importance is the role of interactions between HbS tetramers before the gel has completely materialized which has, till now, with few exceptions, only been speculated upon. The inadequacy of the present state of knowledge is emphasized if we recall that human hemoglobins other than HbS have been observed to aggregate when the in vitro conditions of pH, ionic strength, and Hb concentration are all properly chosen. Aggregation takes the form of amorphous precipitates, polycrystalline structures or gels of fibers, and microtubules (6). Aggregation into a gel of microtubules, under conditions of high salt concentration, has even been observed to occur for oxygenated normal hemoglobin (6). Moreover, it is well known that a hemoglobin found in white-tail deer (HbDIII) will gel in vitro and that the red blood cells of that species will sickle (7). But the in vitro conditions favoring gelation of HbDIII are largely the opposite of those which lead to gelation of HbS. None of these phenomena are at all well understood.

As a step on the road toward a better understanding of the HbS gelling process, some thought it useful to attempt to characterize the pregelation state; i.e., to search for precursors of the gel (8–11). A proof of the existence of such precursors (e.g., dimers and trimers of the basic Hb tetramer) either at equilibrium or as components of some transition state, and a measurement of their size distribution, would be of immediate interest and benefit to gelation theorists.[1] The question of how and indeed whether existing nucleation theories should be applied to the gelling of HbS might be answered by such measurements.

BB. THE METHOD Of the few experimental techniques that have been tried in this area of inquiry, the one that interests us the most and seems currently to show a good deal of promise is intensity fluctuation spectroscopy (IFS). This relatively new technique allows us to measure two quantities: first, the average mutual diffusion coefficient, $\langle D \rangle$, of the Hb molecules in solution; second, the spread in D-values about the average, $\langle (D/\langle D \rangle - 1)^2 \rangle$. The latter quantity is referred to as the (normalized) variance.

---

[1]von Schulthess, G. K. 1979. *In* N-Particle Distributions in Aggregating Systems: Aggregation of Antigen Coated Latex Spheres by Anti-body. Physics Department, Massachusetts Institute of Technology (unpublished thesis). Section 1 of this reference describes several mathematical models of aggregating systems.

More precisely, the IFS experiment measures the time and wave-vector dependent autocorrelation function of the intensity of light scattered at a fixed angle by the solution. For a two component solution (nonscattering solvent plus a solute of monodisperse scatterers), in the single scattering regime ($n^{2/3}\,\sigma \ll 1$, where n is the number density of scatterers and σ is the elastic scattering cross section) and under an assumption of molecular chaos, one finds that:

$$\langle I_q(0)\, I_q(t)\rangle = B + A \cdot \exp(-2q^2Dt).$$

Here, A and B are, broadly speaking, instrumental constants, D is the mutual diffusion coefficient, and $\hbar q$ is the momentum imparted to the scatterer. The simple exponential time-dependence is, in part, a consequence of the assumption of molecular chaos. Note that real systems may not completely satisfy this criterion, especially at high solute concentrations (see section 3Ac).

If the solute is polydisperse, then the correlation function will generally display more than one decay time. The curve fitting procedure extracts both the average inverse decay time, $2q^2D$, and the spread in inverse decay times about the average, $\langle (D/\langle D\rangle - 1)^2\rangle$. The average depicted, $\langle\ \rangle$, involves a weighting over the distribution of scattered intensities (see the Appendix and reference 12).

Existing theories are invoked which relate D to inter- and intramolecular parameters. These theories begin with the Stokes-Einstein relation, valid for a system of solvent plus monodisperse spherical diffusing particles, at infinite particle dilution:

$$D = k_B T/f_0 = k_B T/6\pi\eta_0 R. \tag{1}$$

In Eq. 1, k_B is Boltzmann's constant; T, the absolute temperature; f_0, the friction constant ($f_0 = 6\pi\eta_0 R$ for spherical particles); and η_0, the solvent viscosity. If the diffusing particles are nonspherical, then a more general form of f_0 is required (reference 32; for ellipsoids, the friction constant is known analytically as a function of the major to minor axis ratio). If the solution is nonideal, then hydration of the diffusing particles may occur. In this case, the measured value of R will be increased by an amount equal to the thickness of the hydration shell. Finally, since the solute is monodisperse, $D = \langle D\rangle$, where $\langle D\rangle$ is the average diffusion coefficient measured in the IFS experiment. That the solute is at infinite dilution means that there can be no interaction between solute particles.

More generally, for the case of a monodisperse but interacting solute system, the work of Phillies (20, 21) suggests:

$$D = (\partial\Pi/\partial n)_T \cdot (1 - Vn)/f. \tag{2}$$

In this, the generalized Stokes-Einstein formula, n and V are the concentration ($1/cm^3$) and volume per particle (cm^3), respectively, of the diffusing material, Π is the solution osmotic pressure (concentration-dependent), and f is a friction constant (also concentration-dependent). The factor $(1 - Vn)$ transforms from the solvent-fixed frame, in which the diffusion equation is formulated, to the cell-fixed frame, in which the light-scattering experiment is performed (20). In the limit, as $n \to 0$, one should find that $(\partial\Pi/\partial n)_T \to k_B T$ and $f \to f_0$. Since the solute is monodisperse, $D = \langle D\rangle$.

In the rival theory of Anderson and Reed (29), similar physical assumptions have led to predictions like those of Eq. 2, at small particle concentrations. But, at high concentrations, the predictions of the two theories disagree, with Anderson and Reed's theory describing an

entirely linear dependence of D upon n, and Phillies' theory allowing for a nonlinear behavior. This difference at high concentrations is said to arise from a difference in averaging procedures.

A second rival theory (for interacting solute systems) originates from the membrane diffusion experiments of Keller et al. (30). These experiments have suggested that the mutual diffusion coefficient may be nearly equal to the strongly concentration-dependent tracer or self-diffusion coefficient. It is now widely accepted (27) that the tracer coefficient is represented over the full range of solute concentrations by:

$$D = k_B T/f. \tag{3}$$

However, IFS measurements of mutual diffusion coefficients differ sharply and consistently with the membrane results for both Hb and bovine serum albumin (BSA). The reason for this disagreement is unknown, although it has been argued that the two techniques are measuring fundamentally different things (28).

For a polydisperse solute system (interacting or noninteracting) the diffusion coefficient is a second rank tensor, and neither Eq. 1, 2, nor 3 can be exact. Similarly, for the same reason, it cannot be precisely true that $\langle D \rangle = D$ (with D given by Eqs. 1, 2, or 3). However, for small degrees of polydispersity, it should be true that $\langle D \rangle \approx D$ and Eqs. 1–3 may still be accurate. In such cases, these equations describe the approximate dependence of the principal component of the diffusion tensor upon the dominant particle size (28); i.e., $\langle D \rangle \approx \langle 1/R \rangle$.

We will use Eqs. 1–3 in section 3Aa. Discussion of the IFS variance is deferred to section 3Ac.

BC. IFS/HB: A VIEW OF PAST RESULTS To date, IFS measurements on Hb systems have been reported from several laboratories (9, 13–15). Unfortunately, these data are somewhat inconsistent, with the results varying a bit from laboratory to laboratory. In addition, most of the published studies have been carried out under in vitro conditions which are narrowly defined and somewhat removed from the physiological. The usual choice for the pH is pH $\approx$ pI, and not the physiologically more significant pH = 7.4. Interactions between Hb molecules may be stronger and longer ranged at pH = 7.4, where both HbA and HbS carry net negative charges, than at the pI. Interactions with the solvent may prove to be pH-dependent as well. It is important to realize that, independent of any aggregation which might take place, interactions can have a pronounced effect upon the $\langle D \rangle$ vs. CHb curve (see Figs. 1–5 and discussion in sections 1Bb and 3Aa). Consequently, effects owing to aggregation may be masked. Since the interactions are largely coulombic, their influence can be modified or attenuated through screening by buffer ions. Hence, the ionic strength and perhaps the nature of the buffer are important (Fig. 11). Also, the variance vs. CHb curves can be affected by these factors (Figs. 6–10).

It appears that a study of pregelation aggregation in HbS solutions by IFS at physiological pH must initially aim at improving understanding of the effects of a broad class of interactions; e.g., those interactions which do not necessarily lead to aggregation. This is a subject of great general and current interest (16–18, 20, 21). In summary, it was once reasonable to confine measurements to pH = pI, thus minimizing effects of interactions upon the D-distribution; such investigations should now be seen as a first step. In spite of possible difficulties of data interpretation, a broader range of solution conditions should now be tested.

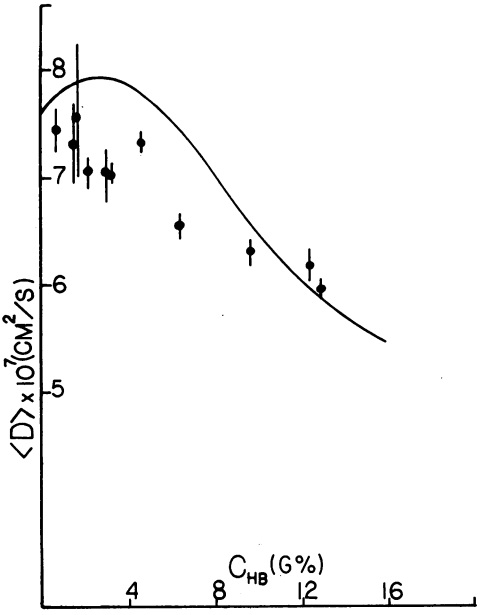

FIGURE 1 $\langle D \rangle$ vs. CHb for oxy-HbA, pH = 6.3, in a 0.05 M potassium phosphate buffer with 0.10 M KCl added; solid curve calculated from Eq. 2 (see section 3Aa).

2. EXPERIMENTAL

A. Sample Preparation

Normal oxy-HbA was prepared according to the following procedure. Blood from human donors was drawn onto a sodium-citrate buffer (blood to buffer volume ratio of 10:1). After packing, the RBC's were washed four times in isotonic saline, then hemolyzed by shaking with one added volume of distilled water and one-half added volume of toluene. The resulting mixture was centrifuged and a clear red Hb solution at a concentration of 10–15% was obtained. The Hb solution was then filtered through No. 2

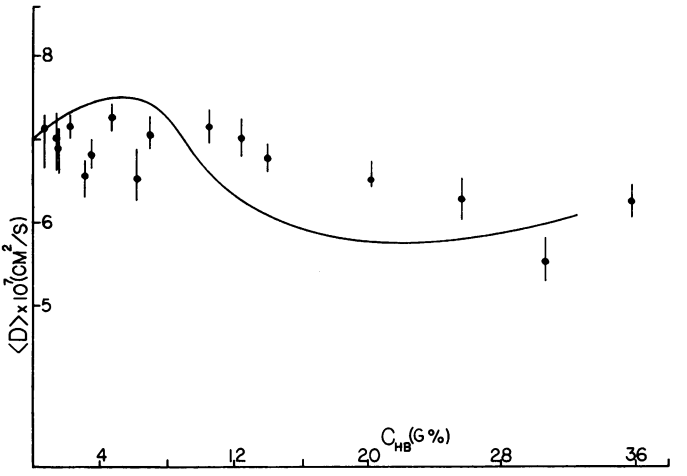

FIGURE 2 $\langle D \rangle$ vs. CHb for oxy-HbA, pH = 6.9; buffer as in Fig. 1; solid curve from Eq. 2.

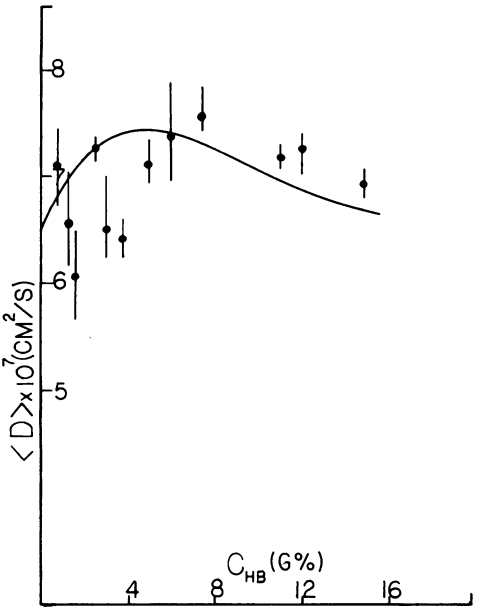

FIGURE 3

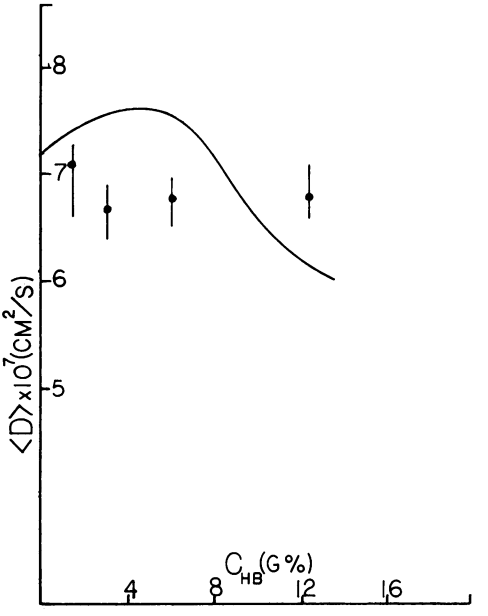

FIGURE 4

FIGURE 3 $\langle D \rangle$ vs. CHb for oxy-HbA, pH = 7.4; buffer as in Fig. 1; solid curve from Eq. 2.
FIGURE 4 $\langle D \rangle$ vs. CHb for oxy-HbS, pH = 6.9; buffer as in Fig. 1; solid curve from Eq. 2.

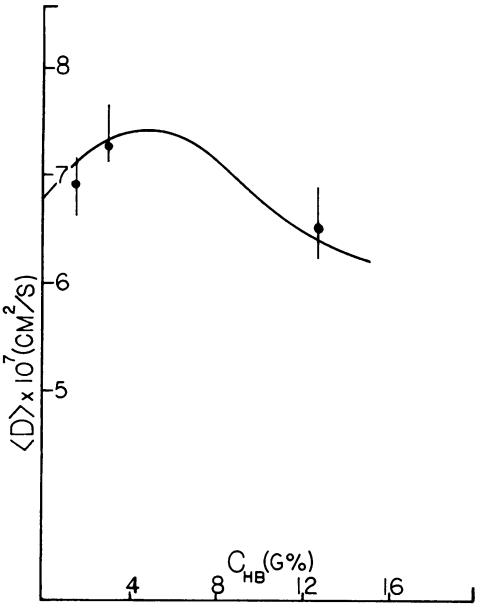

FIGURE 5

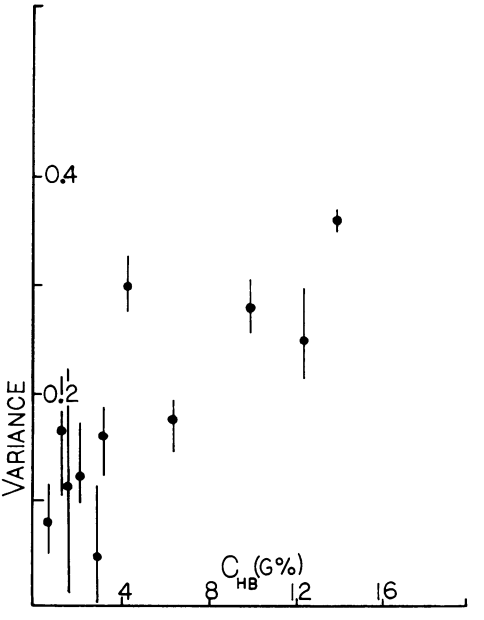

FIGURE 6

FIGURE 5 $\langle D \rangle$ vs. CHb for oxy-HbS, pH = 7.4; buffer as in Fig. 1; solid curve from Eq. 2.
FIGURE 6 Variance vs. CHb for oxy-HbA, pH = 6.3; buffer as in Fig. 1.

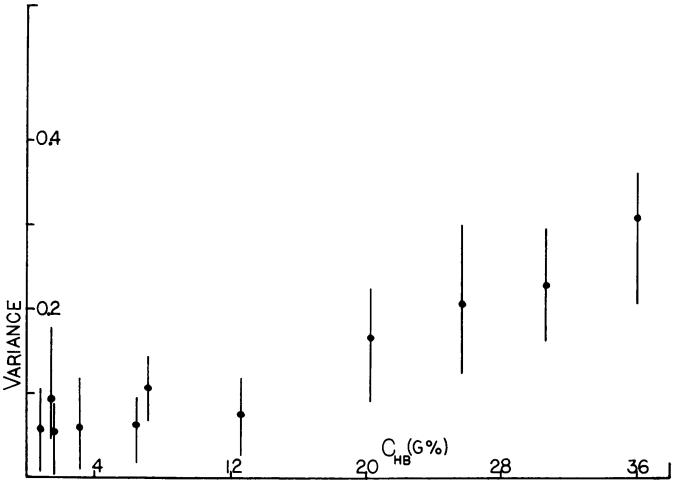

FIGURE 7 Variance vs. CHb for oxy-HbA, pH = 6.9; buffer as in Fig. 1.

filter paper and funneled into dialysis bags. The bags were placed in cold (4°C) stirred distilled water baths for 3 to 5 d, with two or three changes of bath water. The ratio of bath volume to Hb solution volumes was always >100:1. This extensively H_2O-dialyzed Hb had a concentration of ~13%, a pH of ~6.7, and an ionic strength (from measurements of electrical conductivity) of just a few millimolar.

A portion of the H_2O-dialyzed Hb was diluted with solutions of NaCl in water at various ionic strengths; in this way we obtained samples for the measurements recorded in Figs. 11 and 12. The

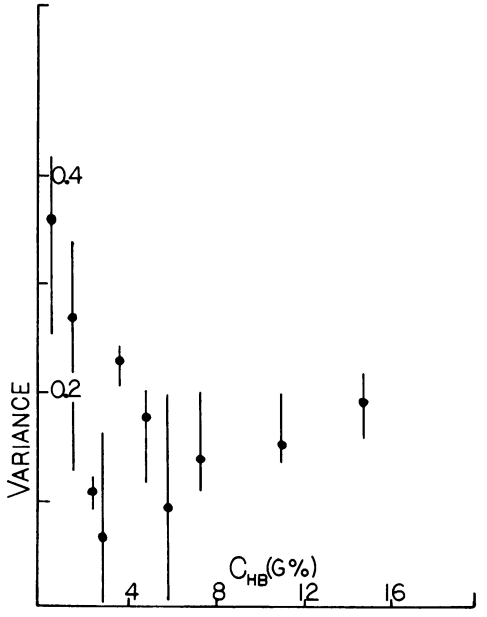

FIGURE 8

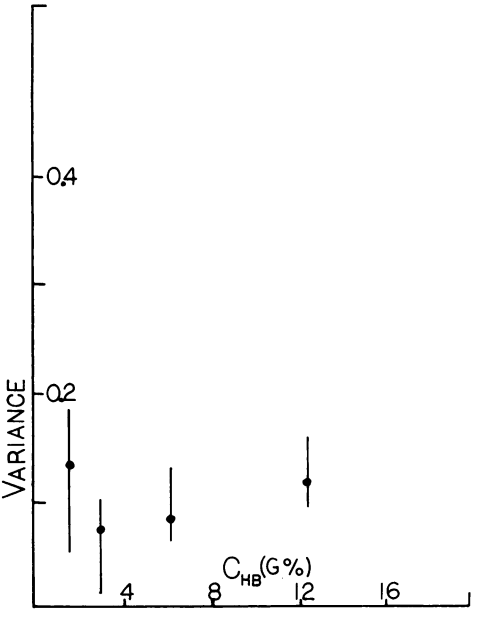

FIGURE 9

FIGURE 8 Variance vs. CHb for oxy-HbA, pH = 7.4; buffer as in Fig. 1.
FIGURE 9 Variance vs. CHb for oxy-HbS, pH = 6.9; buffer as in Fig. 1.

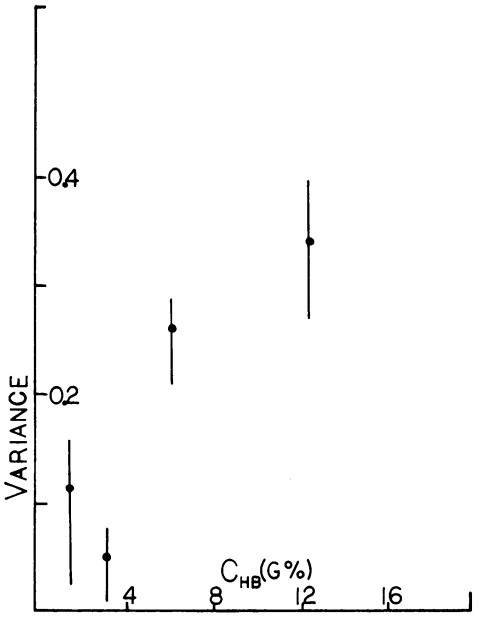

FIGURE 10 Variance vs. CHb for oxy-HbS, pH = 7.4; buffer as in Fig. 1.

remainder of the H_2O-dialyzed Hb was redialyzed against a 0.05 M potassium phosphate buffer containing 0.10 M KCl. Material emerging from this second dialysis was used to prepare samples for the measurements recorded in Figs. 1–10. The buffer dialysis proceeded for 2 d at 4°C, with the ratio of buffer volume to sample volume of >100:1. A portion of the buffer bath was filtered through No. 2 filter paper and was used to prepare samples at various concentrations by dilution. After removing each Hb solution from its dialysis bath, visible absorption spectra were recorded on a Cary-14R spectrophotometer (Cary Instruments, Fairfield, N.J.). The concentrations of oxy-Hb and of Met-Hb were determined by absorption measurements at 577 and 630 nm, respectively. The fraction of Met-Hb never exceeded

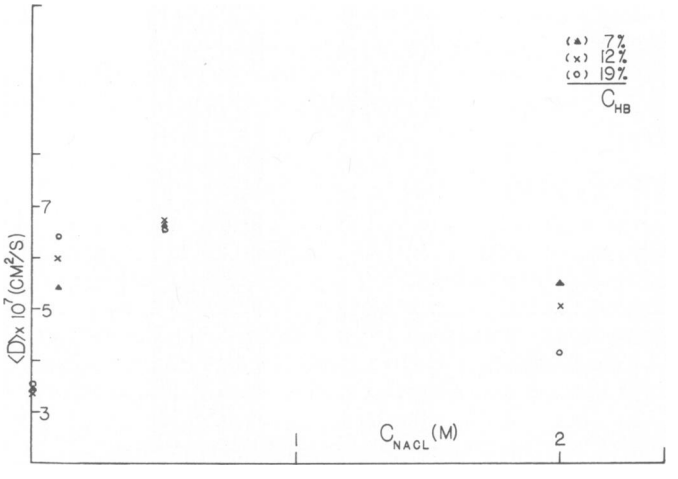

FIGURE 11 $\langle D \rangle$ vs. CNaCl for oxy-HbA, pH = 6.7, at various values of CHb.

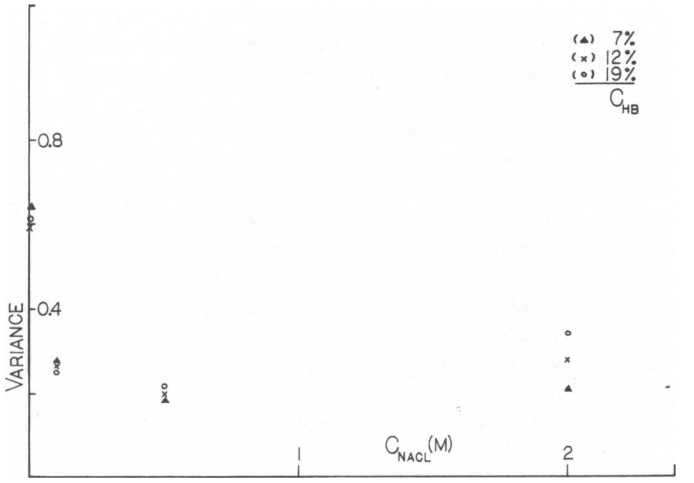

FIGURE 12 Variance vs. CNaCl for oxy-HbA, pH = 6.7, at various values of CHb.

0.03 of the total Hb present. (Millimolar extinction coefficients were taken to be 15.37 for oxy-Hb at 577 nm, and 3.70 for Met-Hb at 630 nm.) Hb solutions at Chb $\gtrsim$ 13% were prepared by first concentrating to a maximum CHb of ~35% in an Amicon concentrator (Amicon Corp., Lexington, Mass.), then diluting with buffer. The Amicon concentration of Hb was achieved at a temperature of 4°C under nitrogen at a pressure of 25 p.s.i.

The various Hb solutions were prepared from the dialyzed samples of Hb by dilution with the appropriate buffers and salt solutions in 1/2-ml glass culture tubes. The tubes had been cleansed by boiling in dilute solutions of ethanol and distilled water, then rinsed repeatedly, and finally dried in an oven. The dilutions were all performed in cold culture tubes with a Pipetteman of maximum volume 200 λ equipped with disposable plastic tips. The culture tubes containing the various Hb solutions were spun at 10,000 *g* for 1 h in a refrigerated centrifuge. Immediately after centrifugation an aliquot of each Hb solution was drawn from the very top of each culture tube into a 100-λ glass capillary. These 100-λ capillaries were the actual sample holders used for the IFS measurements. The filled capillaries were sealed with wax at both ends (the wax did not touch the Hb solutions) and the finished samples were stored at 4°C. less than 4 d were allowed to elapse between the removal of samples from dialysis (at which time absorption spectra were taken) and the actual IFS measurements.

Oxy-HbS samples were prepared as described for oxy-HbA, except that the homozygous SS blood was drawn onto an EDTA anticoagulant. Results of measurements made on these samples appear in Figs. 4, 5, 9, and 10.

B. IFS Measurements

The samples prepared as described were placed singly into a temperature controlled sample oven situated at the laser focus. All measurements were performed with the sample oven temperature preset to 23°C. Estimates showed negligible temperature rise in the capillary owing to heating of the protein by the laser for the samples chosen. A 5-mW He-Ne laser was used (Spectra-Physics Inc., Mountain View, Calif.; model 120) operating at a wavelength of 632.8 nm in a polarized TEM00 mode. The laser and associated optics, the photomultiplier tube, the sample oven, and all power supplies and controllers were contained in a single modular unit assembled and made available by Nicomp Instruments (Santa Barbara, Calif.). The autocorrelation function of the intensity of light scattered through 90° was computed on-line by a Nicomp Instruments computing autocorrelator. As an added feature this particular device computes the first two moments of the *D*-distribution automatically. Instrument calibration was checked by performing IFS measurements of the diffusion coefficients of submicron size

latex spheres (supplied by Dow Chemical Co., Diagnostic Products Div., Midland, Mich.). Very dilute solutions of spheres were measured to minimize the effects of multiple-scattering. Sphere radius was calculated from Eq. 1 and found to be in good agreement with the value claimed by Dow. The IFS variance for these spheres was $\lesssim 0.05$.

Owing to our use of the capillary as sample holder, the optical pathlength was a mere 0.3 mm and attenuation of the incident beam by absorption was never a limiting factor; i.e., no problem was encountered with obtaining sufficient scattered intensity, even at the highest Hb concentrations. If, instead, a standard 1-cm pathlength cuvette had been used, no useful data could have been obtained unless the laser had been focused at or very near the edge of the cuvette.

Several IFS measurements were made on each of the Hb samples. The average of the experimentally determined $\langle D \rangle$ values and the average of the variances appear in Figs. 1–12. Error bars, where included, are meant to reflect the range of measured values.

Lastly, we mention that the data reported for oxy-HbA have been checked for reproducibility by repeating the entire procedure with blood drawn from a different donor. Only minor differences exist between the data taken in these two different sets of experiments.

3. RESULTS AND DISCUSSION

A. pH $\gtrless$ pI; Fixed Ionic Strength (Γ = 0.15 M)

AA. $\langle D \rangle$ VS. CHB FOR OXY-HBA We begin this section with a summary of its contents: (*a*) The volume of water bound to Hb is deduced from the value of $\langle D \rangle$, at CHb $\rightarrow$ 0, for each pH. The possibility of an error at this point due to particle asymmetry is considered. (*b*) Osmotic pressure vs. CHb curves are computed from the virial expansion. A modified form of hard sphere interaction between tetramers is proposed. The volume of the invoked hard sphere includes the experimentally determined hydration volume. (*c*) A curve of solution viscosity vs. CHb is derived from published Hb tracer diffusion data. It is assumed that the viscosity is independent of the degree of Hb hydration. (*d*) Using *a-c* and the generalized Stokes-Einstein formula, curves of $\langle D \rangle$ vs. CHb are calculated. At every pH, a good agreement with the experimental data is obtained.

We now consider these four points in more detail. In the limit, as CHb $\rightarrow$ 0, $\langle D \rangle$ becomes a direct measure of the average particle size. This follows from Eq. 1 (assuming both a small degree of polydispersity and either spherical particles or particles of a known asymmetry). Referring to our data of Figs. 1–3, one sees that as the pH varies a pronounced change in $\langle D \rangle$ occurs at the small CHb values. At pH = 6.3 (Fig. 1), the small CHb limit of $\langle D \rangle = 7.6 \times 10^{-7}$ cm^2/s implies an average radius of $\langle R \rangle$ = 30.5 Å; at pH = 6.9, $\langle R \rangle$ = 33.1 Å (Fig. 2), and $\langle R \rangle$ = 35.7 Å at pH = 7.4 (Fig. 3). We ascribe these changes in average radius to changes in the degree of particle hydration. If this interpretation is correct, then at pH values of 6.3, 6.9, and 7.4 an oxy-HbA tetramer carries 1, 2, and 3 monolayers of bound water, respectively. (We assume that $\langle 1/R \rangle = 1/\langle R \rangle$ and that the particles are spherical.) Alternatively, the particle asymmetry may be increasing as the pH rises, with the degree of hydration remaining fixed. However, considering the size of the observed changes, this seems to be an unlikely hypothesis. The observed effect is probably the result of a combination of causes, wherein degree of hydration plays the most important part.

At elevated particle concentrations, CHb > 0, one sees evidence of a marked dependence of $\langle D \rangle$ upon both pH and upon CHb. At pH < pI (Fig. 1), the $\langle D \rangle$ vs. CHb curve falls continuously as CHb increases; for pH $\approx$ pI (Fig. 2), the $\langle D \rangle$ vs. CHb curve is first nearly flat, then falls for CHb $\gtrsim$ 12%; and for a pH > pI (Fig. 3), the $\langle D \rangle$ vs. CHb curve first rises

to a maximum, then falls for CHb $\gtrsim$ 6%. The data of Fig. 2 are in close agreement with reference 13 and fair agreement with reference 15 if the data in these two papers are adjusted to 23°C.

For BSA a similar behavior of the $\langle D \rangle$ vs. C curves at pH $\gtrless$ pI, and for intermediate values of ionic strength, has been reported (19). An attempt was made by those workers to match their data with the predictions of the generalized Stokes-Einstein relationship (our Eq. 2). Although, in general, only qualitative agreement between theory and experiment was obtained, the three most striking features of the data were fit rather accurately. Namely, that for pH < pI the curve of $\langle D \rangle$ vs. CBSA fell monotonically with increasing CBSA; for pH $\approx$ pI the $\langle D \rangle$ vs. CBSA curve was nearly flat over the whole CBSA range; and for pH > pI, the $\langle D \rangle$ vs. CBSA curve first rose to a maximum as CBSA increased, then declined slightly for values of CBSA $\gtrsim$ 10%. In these calculations, the friction constant, f, was assumed to be inversely proportional to the tracer diffusion coefficient and independent of pH (see our Eq. 3). The tracer diffusion coefficient was taken from the measurements of Keller et al. (30) and the osmotic pressure data were those of Scatchard (31).

Eq. 2 has also been used in the interpretation of $\langle D \rangle$ vs. CHbA data (13, 14). In reference 13, tracer coefficients taken from experiment were combined with calculated values of osmotic pressure (hard sphere potentials invoked). In reference 14, the friction constant, f, was assumed to be directly proportional to the solution viscosity, and both the viscosity and osmotic pressure were measured. In reference 14, the theory fit the data rather well. But in reference 13 it was necessary to introduce a correction to the generalized Stokes-Einstein formula (said to be owing to hydrodynamic effects). The work of references 13 (cyanomet-HbA, pH = 7.2) and 14 (oxy-HbA, pH $\approx$ pI) was all performed at intermediate values of the ionic strength.

Inasmuch as our experimental data exhibit nonlinear variations of $\langle D \rangle$ with CHb, we have confined our attention to the predictions of Eq. 2 (Phillies' theory). In Figs. 1–3 we plot (solid lines) values of $\langle D \rangle$ vs. CHb as computed from this equation. The tracer diffusion data of Keller et al. (30) were used to deduce the concentration dependence of the friction constant, f. These data (cyanomet-HbA into met-HbA at pH = 7.7 and T = 25°C) were assumed to be independent of the Fe oxidation state and of the nature of the bound ligand. No correction was made for the slight difference in temperature between Keller's experiment and ours (a difference of 2°C). It is proposed that the trapping of water within the hydration shells does not affect the solution viscosity; i.e., at fixed CHb, η does not depend upon the degree of Hb hydration. This seems a plausible hypothesis, but remains unproved.

The derivative of osmotic pressure with respect to concentration was obtained from the CS theory for a system of hard spheres (23):

$$(\partial \Pi / \partial n)_T = k_B T(1 + 4\theta + 4\theta^2 - 4\theta^3 + \theta^4)/(1 - \theta)^4. \tag{4}$$

Here, n is the concentration of diffusing particles ($1/cm^3$) and θ is their volume fraction (volume of diffusing material per unit volume of solution). Eq. 4 is expected to hold for hard sphere systems of $\theta \lesssim 0.5$. (For a simple cubic lattice of spheres $\theta = 0.52$.) θ was determined at each pH from the formula:

$$\theta = gC/100\rho. \tag{5}$$

TABLE I
pH DEPENDENCE

pH	$\langle R \rangle$	C/CHb	ρ	Z
	(Å)		(g/ml)	
6.3	30.5	1.364	1.227	+1.23
6.9	33.1	1.673	1.177	−0.39
7.4	35.7	2.035	1.141	−1.85

Here, C is the concentration of diffusing particles (grams percent) and ρ is their mass density (grams per milliliter). The dimensionless factor g corrects for deviations from pure hard sphere behavior ($g \sim 1$). Since, under the conditions of our experiment, the Debye screening length is small ($\lambda_D = 1.25$ Å, at $\Gamma = 0.15$ M), the hard sphere model should have substantial validity.

Because of the variation of the degree of Hb hydration with pH, the particle density ρ and the ratio C/CHb are both nontrivial functions of pH. Assuming a dry density value for oxy-HbA of 1.333 g/ml (24) and assuming that diffusing particles are spherical, then values of ρ and C/CHb follow from a knowledge of the experimentally determined $\langle R \rangle$. These results are summarized in Table I. Over the range of pH values considered, the pH-dependence of θ is given to a good approximation by:

$$\theta = g(0.01366 - 0.00217Z)\text{CHb}, \tag{6}$$

with CHb in grams percent. Z is the titration charge of oxy-HbA (22). The frame transformation factor (Eq. 2) is,

$$(1 - Vn) = (1 - C/100\rho). \tag{7}$$

The correction factor, g, was selected with a view toward obtaining the best fit of Eq. 2 to the experimental data of Figs. 1–3. The value resulting in this best fit was $g = 0.60$, independent of pH. We conclude that the hard sphere model is basically sound, but that the contact radius is less than the hydrodynamic radius, R, by $(1 - 0.60^{1/3})R$. This amounts to ~5 Å, or about one monolayer of adsorbed water, at all pH values considered. The discrepancy could be the result of a collision-induced distortion of the shells of bound water. Since water is essentially incompressible, this suggests a process of flow within the hydration shell away from regions of interparticle contact. A second possibility, that the diffusing particles are manifestly nonspherical, can be ruled out since, for nonspherical particles, $g > 1$ (23). Still a third possibility is that $g = 1$, but that hydrodynamic effects (13) act to further complicate the description. Indeed, the hydrodynamic effects can be included (at the expense of introducing a new adjustable parameter) and good agreement with our experimental data can be obtained. We do not favor this approach, however, for the following reason. We have compared the predictions of Eq. 4, integrated once with respect to CHb, and Eq. 6 ($g = 0.60$) with the Π vs. CHb data of Adair (reference 26; this data is for oxy-Hb at pH = 7.7 and $\Gamma = 0.15$ M). Our calculated values of Π agree quite well with these experimental data over the entire range of Hb concentrations $0 < \text{CHb} < 32\%$. Contrariwise, if $g = 1$, only poor agreement with Adair's data is obtained.

It is interesting to note, again, the similarity between our result and the result of reference

19 for BSA. In both cases a linear dependence of the second virial coefficient upon titration charge is found. Scatchard (31), whose osmotic pressure data strongly support the BSA results, has speculated that the effect is caused by a hydration of the BSA molecules. However, he was unable to verify that conjecture since he had no means of determining particle size directly.

AB. $\langle D \rangle$ VS. CHB FOR OXY-HBS In Fig. 4 we plot $\langle D \rangle$ vs. CHb for oxy-HbS at pH = 6.9. In Fig. 5 the same variables are plotted, but at pH = 7.4. These data are self-consistent and consistent with the data of Figs. 1–3 if allowance is made for the fact that the pI of oxy-HbS is slightly higher than that of oxy-HbA (by ~0.2 pH units (1)). Also, in these two figures we plot (solid lines) the results of a calculation of $\langle D \rangle$ based upon Eq. 2, the generalized Stokes-Einstein formula. We use Eq. 6 and estimated values of Z. The procedure is described completely in section 3Aa.

AC. VARIANCE VS. CHB Perhaps because no existing theory predicts the behavior of the variance vs. CHb, these curves are usually not reported (an exception is the paper of Jones and Johnson (15) describing the IFS measurements on oxy-HbA and oxy-HbS at pH $\approx$ pI. It is certainly not the case that these curves are uninteresting owing to a lack of discernible structure or, in general, to a lack of reproducibility. A brief study of Figs. 6–10 makes this clear. At pH = 6.3 the variance increases rapidly for oxy-HbA (Fig. 6): at pH = 6.9, very slowly for oxy-HbA and oxy-HbS; (Figs. 7 and 9; this result is in accord with reference 18); and at pH = 7.4, rapidly for oxy-HbS (Fig. 10) and oxy-HbA (Fig. 8; for CHb $\gtrsim$ 5%). It is probably significant that larger values of the variance are associated with smaller values of $\langle D \rangle$; e.g., Figs. 8 and 3 at small values of the CHb. Also, see Figs. 6 and 1 at the larger CHb values.

A few general remarks seem to be in order. In polydisperse systems the IFS variance reflects the spread in particle sizes about the mean. If the system is noninteracting, then the variance measures polydispersity only. However, for an interacting system, the variance may reflect the existence of persistent correlations, too. These correlations are of a sort not contemplated by the classical fluid theory (of Enskog) but have been shown to exist, even in hard sphere systems (23). They may contribute to the IFS variance since they may cause the solution density autocorrelation function to depart from a simple exponential time dependence. This departure may result in a lowering of the measured $\langle D \rangle$-value as well as an increase in the variance. The effect is expected to be strongly concentration-dependent, occurring much more noticably at high solute concentrations.

It is interesting to note that the variance measured at pH = 6.9 (Fig. 7) is minimal until rather large CHb values are reached. However, at pH = 6.3 (Fig. 6) the variance rises steeply, even for small CHb values. This behavior should be viewed in the light of the preceding remarks, bearing in mind that interactions at pH = 6.3 may be more extensive than at pH = 6.9 (the pI). The data of Fig. 8, at pH = 7.4, exhibit two different trends. First, there is a rise in the variance, beginning at intermediate CHb values. This may be the result of persistent correlations. Second, for small CHb values, the variance increases as CHb approaches zero. This is a puzzling effect, for which we have no likely explanation.

B. Fixed pH (pH $\approx$ 6.7); Ionic strength Varied

We turn now to the results of measurements made on unbuffered oxy-HbA solutions at various levels of salt at or near pH = 6.7 (self-buffering by the protein holds the pH near 6.7

as the ionic strength is varied). In Fig. 11 we plot $\langle D \rangle$ vs. CNaCl for several fixed CHb values. As is seen, the shape of the curves is insensitive to the value of CHb over the range of CHb values treated. A similar remark applies to the variance vs. CNaCl curves of Fig. 12. We note that $\langle D \rangle$ has a maximum and the variance a minimum in the vicinity of CNaCl $\approx$ 0.3–0.5 M. The simplest interpretation of these data assigns them as evidence of a clustering of HbA tetramers, under conditions of both very low and very high salt. Based upon the data, a quantitative estimate of the friction constant of a diffusing cluster, at millimolar values of CNaCl, yields $f = 10f_0/3$. Here, $f_0 = 6\pi\eta R$ is the friction constant of a single Hb tetramer and R is its hydrodynamic radius. If the clusters are spherical, then the ratio of the number of clusters of tetramers to the number of free tetramers is ~0.002, the number of tetramers per cluster if ~25, and the cluster radius is ~90 Å. About 6% of the total Hb is formed into clusters. If the clusters are nonspherical then the number of tetramers per clusters is reduced. The amount of Hb incorporated into clusters will probably be reduced. The details of this calculation may be found in the Appendix.

For completeness, we mention that for BSA (25), at pH = pI, the curve of $\langle D \rangle$ vs. CSalt is flat over a range of CSalt values extending from millimolar to molar. At pH < pI, $\langle D \rangle$ rises rapidly as CSalt falls into the millimolar range, owing presumably to the increasing strength of repulsive coulomb interactions between the increasingly unscreened protein (net positive) charges. This distinctly different behavior in BSA, under conditions where the protein is expected to remain essentially monomeric, lends credence to the hypothesis of clustering in the Hb system.

4. CONCLUSIONS

It has been established that much interesting structure exists in the curves of $\langle D \rangle$ and the variance vs. CHb for oxy-HbA and oxy-HbS. A considerable success in the understanding of this structure has been achieved. In particular, the generalized Stokes-Einstein formula (Eq. 2) has been shown to make rather accurate predictions of the curves of $\langle D \rangle$ vs. CHb, for $6.3 \leq$ pH ≤ 7.4, at $\Gamma = 0.15$ M. This formula is a very obvious improvement over the ordinary Stokes-Einstein relation (Eq. 1), since the ordinary relation is concentration-independent and cannot describe the effects seen in Figs. 1–5. The generalized Stokes-Einstein formula is an improvement over Eq. 3, since the tracer diffusion coefficient is known to fall monotonically and rapidly with increasing protein concentration and cannot describe the effects depicted in Figs. 2–5. Lastly, the generalized Stokes-Einstein formula is able to mimic the observed nonlinear dependence of $\langle D \rangle$ upon CHb, in contrast to the theory of Anderson and Reed (29), which predicts a purely linear behavior.

A pronounced pH dependence of $\langle D \rangle$, at CHb $\rightarrow$ 0, has been observed. This was attributed to a pH-dependent change in the degree of Hb hydration. We have suggested that the mass of the hydration shell increases monotonically as the pH rises, for $6.3 \leq$ pH ≤ 7.4. Past measurements of the complex dielectric constant of Hb solutions may have exhibited this effect (33).

The discovery of aggregation in oxy-HbA solutions at very low salt is interesting in that it gives further evidence of the ability of normal Hb to undergo intertetrameric bonding. It may be only a coincidence that the IFS (average) diameter of oxy-HbA aggregates (see section 3B) is comparable to the diameters of Hb microtubules seen in electron micrographs (6).

We point out that the interpretations of these IFS data should be viewed in the context of our having failed to account quantitatively for the curves of variance vs. CHb. In view of the apparent close connection between $\langle D \rangle$ and $\langle (D/\langle D \rangle - 1)^2 \rangle$, a caveat is in order.

We conclude by calling attention to the correlation between several of the features of the curves of $\langle D \rangle$ and variance vs. CHb for oxy-HbA and oxy-HbS (see Fig. 2 and 4 and the similarity between Figs. 7 and 9). This has been remarked upon already in section 3Ab. We ascribe this correlation to the close similarity of these two Hb species, both as to overall size and shape, and as to type and strength of intermolecular interaction, under the conditions considered. This observation is based upon data taken at values of CHb $\lesssim$ 12%. At higher concentrations the similarity between oxy-HbA and oxy-HbS may not persist. Clearly, data taken at higher concentrations would be desirable and more relevant to the sickling problem.

It will also be of very considerable interest to extend this work to deoxy-HbA and deoxy-HbS, and to compare the results obtained from measurements made on those systems with each other and with the corresponding oxy-Hb results. Preliminary work on deoxy-Hb has shown that our experimental technique is easily adapted to that more demanding system.

Dr. LaGattuta wishes to thank Professor R. Schor of the Department of Physics, University of Connecticut, for useful discussions.

This work was supported by a National Research Service Award (National Institutes of Health [NIH] grant AM07233) held by Dr. LaGattuta and by NIH grants AM18781 and AM17348. Experiments were carried out during the summer and fall of 1979. All samples were prepared in the Hemoglobin Research Lab of the Department of Medicine, University of California at San Diego. IFS measurements were performed in the laboratories of the Department of Physics, University of California at Santa Barbara.

Received for publication 29 July 1980 and in revised form 18 September 1980.

APPENDIX

We assign the data of Figs. 11 and 12 as evidence of Hb clustering at extremely low concentrations of salt. Assuming a bimodal distribution of particle sizes, an estimate of the extent of aggregation is obtained as follows. Since the IFS average is an intensity weighted average (12) and the scattering is in the Rayleigh regime,

$$I_j \propto n_j V_j^2 \tag{A1}$$

$$\langle D \rangle = (D_1 I_1 + D_2 I_2)/(I_1 + I_2) \tag{A2}$$

$$\langle D^2 \rangle = (D_1^2 I_1 + D_2^2 I_2)/(I_1 + I_2). \tag{A3}$$

In Eq. A1, n_j, V_j, and I_j are the concentration ($1/cm^3$), volume per particle, and scattered intensity, respectively, of the jth species (j - 1, 2). In Eqs. A2 and A3, the intensity average is applied. We use a suffix 1 to denote an Hb tetramer and a suffix 2 to denote an aggregate of tetramers.

The data of Figs. 11 and 12 show that,

$$\langle D \rangle / D_1 = 0.5 \tag{A4}$$

$$\langle (D/\langle D \rangle - 1)^2 \rangle = 0.4. \tag{A5}$$

Substituting Eqs. A4 and A5 into Eqs. A2 and A3, and solving for the ratio D_2/D_1 yields,

$$D_2/D_1 = 0.30. \tag{A6}$$

Then, using Eqs. A2–A6 and assuming $D_j \propto 1/R_j$ one finds that,

$$n_2/n_1 = 0.00182, \tag{A7}$$

and that the fraction of aggregated material is,

$$n_2V_2/(n_1V_1 + n_2V_2) = 0.06. \tag{A8}$$

The radius of the cluster is,

$$R_2 = 10R_1/3 \approx 90 \text{ Å}, \tag{A9}$$

and the number of tetramers per cluster is ~25 (assuming a body-centered cubic packing of spherical tetramers).

It should be realized that these results depend upon the assumption of spherical clusters. If the cluster is asymmetric, then the number of Hb tetramers per cluster is reduced.

REFERENCES

1. PAULING, L., H. A. ITANO, S. J. SINGER, and I. C. WELLS. 1949. Sickle cell anemia, a molecular disease. *Science (Wash. D.C.).* **110**:543–548.
2. RANNEY, H. M. 1973. Summary of the Symposium. *In* Sickle Cell Disease. H. Abramson, J. F. Bertles, and D. L. Wethers, editors. C. V. Mosby Co., St. Louis. 315–325.
3. MURAYAMA, M., and R. M. NALBANDIAN. 1973. Sickle Cell Hemoglobin Molecule To Man. Little Brown and Co., Boston. 41.
4. MAGDOFF-FAIRCHILD, B., and C. C. CHIU. 1979. X-ray diffraction studies of fibers and crystals of deoxygenated sickle cell hemoglobin. *Proc. Natl. Acad. Sci. U.S.A.* **76**:223–226.
5. NAGEL, R. L., R. N. BOOKCHIN, J. JOHNSON, D. LABIE, H. WAJCMAN, W. A. ISSAC-SODEYE, G. R. HONIG, G. SCHILIRO, J. H. CROOKSTON, and K. MATSUTOMO. 1979. Structural bases of the inhibitory effects of hemoglobin F and hemoglobin A_2 on the polymerization of hemoglobin *S*. *Proc. Natl. Acad. Sci. U.S.A.* **76**:670–672.
6. WHITE, J. G., and B. HEAGAN. Fine structure of hemoglobin polymerization. *In* Sickle Cell Disease. H. Abramson J. F. Bertles, and D. L. Wethers, editors. C. V. Mosby Co., St. Louis. 104–129.
7. GIRLING, R. L., W. C. SCHMIDT, JR., T. E. HOUSTON, and E. L. AMMA. 1979. Molecular packing and intermolecular contacts of sickling deer type III hemoglobin. *J. Mol. Biol.* **131**:417–433.
8. LINDSTROM, T. R., S. H. KOENIG, T. BOUSSIOS, and J. F. BERTLES. 1976. Intermolecular interactions of oxygenated sickle hemoglobin molecules in cells and cell-free solutions. *Biophys. J.* **16**:679-689.
9. WILSON, W. W., M. R. LUZZANA, J. T. PENNISTON, and C. S. JOHNSON, JR. 1974. Pregelation aggregation of sickle cell hemoglobin. *Proc. Natl. Acad. Sci. U.S.A.* **71**:1260–1263.
10. WILLIAMS, R. C., JR. 1973. Concerted formation of the gel of hemoglobin S. *Proc. Natl. Acad. Sci. U.S.A.* **70**:1506–1508.
11. ELBAUM, D., R. L. NAGEL, and T. T. HERSKOVITS. 1976. Aggregation of deoxyhemoglobin S at low concentrations. *J. Biol. Chem.* **251**:7657–7660.
12. CUMMINS, H. Z. 1974. Applications of light beating spectroscopy to biology. *In* Photon Correlation and Light Beating Spectroscopy. H. Z. Cummins and E. R. Pike, editors. Plenum Press, New York. 285–324.
13. ALPERT, S. S. and G. BANKS. 1976. The concentration dependence of the hemoglobin mutual diffusion coefficient. *Biophys. Chem.* **4**:287–296.
14. VELDKAMP, W. B., and J. R. VOTANO. 1976. Effects of intermolecular interaction on protein diffusion in solution. *J. Phys. Chem.* **80**:2794–2801.
15. JONES, R. C., and C. S. JOHNSON, JR. 1978. Photon correlation spectroscopy of hemoglobin: diffusion of oxy-HbA and oxy-HbS. *Biopolymers.* **17**:1581–1593.
16. DOHERTY, P., and G. B. BENEDEK. 1974. The effect of electric charge on the diffusion of macromolecules. *J. Chem. Phys.* **61**:5426–5434.
17. WEISSMAN, M. B., and B. R. WARE. 1977. Applications of fluctuation transport theory. *J. Chem. Phys.* **68**:5069–5076.
18. RAMAN, K., and R. SCHOR. 1976. Effects of ionic charge on light scattering by macromolecules in solution. *J. Chem. Phys.* **66**:1837–1841.

19. PHILLIES, G. D. J., G. B. BENEDEK, and N. A. MAZER. 1976. Diffusion in protein solutions at high concentrations: a study of quasielastic light scattering spectroscopy. *J. Chem. Phys.* **65**:1883–1892.
20. PHILLIES, G. D. J. 1975. Continuum hydrodynamic interactions and diffusion. *J. Chem. Phys.* **62**:3925–3932.
21. PHILLIES, G. D. J. 1974. Effects of macromolecular interactions on diffusion. I. Two-component solutions. *J. Chem. Phys.* **60**:976–982.
22. ANTONINI, E., and M. BRUNORI. 1971. Hemoglobin and myoglobin in their reactions with ligands. *Front. Biol.* **21**:1–111.
23. BARKER, J. A., and D. HENDERSON. 1976. What is liquid? Understanding the states of matter. *Rev. Mod. Phys.* **48**:587–671.
24. ROSSI-FANELLI, A., E. ANTONINI, and A. CAPUTO. 1964. Hemoglobin and myoglobin. *Adv. Prot. Chem.* **19**:73.
25. RAJ, T., and W. H. FLYGARE. 1974. Diffusion studies of bovine serum albumin by quasielastic light scattering. *Biochemistry.* **13**:3336–3340.
26. ADAIR, G. S. 1929. The thermodynamic activities of the proteins. *Proc. Roy. Soc. Lond.* **51**:696–707.
27. ALDER, B. J., D. M. GASS, and T. E. WAINWRIGHT. 1970. Studies in molecular dynamics. VIII. The transport coefficients for a hard-sphere fluid. *J. Chem. Phys.* **53**:3813–3826.
28. PHILLIES, G. D. J. 1974. Effects of macromolecular interaction on diffusion. II. Three-component solutions. *J. Chem. Phys.* **60**:983–989.
29. ANDERSON, J. L., and C. C. REED. 1976. Diffusion of spherical macromolecules at finite concentration. *J. Chem. Phys.* **64**:3240–3250.
30. KELLER, H. K., E. R. CANALES, and S. I. YUM. 1971. Tracer and mutual diffusion coefficients of proteins. *J. Phys. Chem.* **75**:379–387.
31. SCATCHARD, G., A. C. BATCHELDER, and A. BROWN. 1946. Preparation and properties of serum plasma proteins. VI. Osmotic equilibria in solutions of serum albumin and sodium chloride. *J. Am. Chem. Soc.* **68**:2320–2329, 2610–2612.
32. TANFORD, C. 1961. Physical Chemistry of Macromolecules. John Wiley & Sons, Inc., New York. 327.
33. VON CASIMIR, W., N. KAISER, F. KEILMANN, A. MAYER, and H. VOGEL. 1968. Dielectric properties of oxyhemoglobin and deoxyhemoglobin in aqueous solution at microwave frequencies. *Biopolymers.* **6**:1705–1715.